Diatom Adhesion and Motility

Nicole Poulsen, Metin Gabriel Davutoglu, and Jirina Zackova Suchanova

Abstract

Diatoms live in a diverse range of aquatic habitats with species being either free floating (planktonic) or attached to underwater structures (benthic). Ancestrally, diatoms are thought to have been planktonic with nonmotile vegetative cells and motile, flagellated cells for sexual reproduction. The single loss of motile, flagellated gametes in the common ancestor of pennate diatoms was a significant evolutionary step that was associated with the development of active motility in vegetative cells, which enabled outcrossing and their migration into previously inaccessible habitats (Nakov et al., Accelerated diversification is related to life history and locomotion in a hyperdiverse lineage of microbial eukaryotes (Diatoms, Bacillariophyta). New Phytol 219:462–473, 2018). The motility of benthic diatoms allows cells to actively maintain their position in the photic zone, avoid desiccation (e.g., during tidal fluctuations), identify optimal nutrient conditions, and perform sexual mating. The ability of motile diatoms to actively respond to changing environmental conditions provides a substantial selective advantage. Therefore, the evolution of migration ability is believed to be one of the reasons for diatom success and high rates of diversification in benthic habitats. In this chapter, we will review the current literature on the mechanism of cell motility, the extracellular signals that mediate cell motility, and the molecular composition of diatom adhesives.

Keywords

Diatom · Adhesion · Motility · Migration · Benthos

N. Poulsen (✉) · M. G. Davutoglu · J. Zackova Suchanova
B CUBE – Center for Molecular Bioengineering, Technical University of Dresden, Dresden, Germany
e-mail: nicole.poulsen@tu-dresden.de

A. Falciatore, T. Mock (eds.), *The Molecular Life of Diatoms*,
https://doi.org/10.1007/978-3-030-92499-7_14

Abbreviations

AFM	atomic force microscopy
AMC	adhesion motility complex
BDM	2,3-Butanedione monoxime
dP	dissolved orthophosphate
dSi	dissolved silicic acid
EM	electron microscopy
EPS	extracellular polymeric substance
F-actin	filamentous actin
GFP	green fluorescent protein
lux	luminous flux per unit area
PAM	Pulse-Amplitude-Modulation
SEM	scanning electron microscopy
SIP	sex-inducing pheromone
TEM	transmission electron microscopy
PTS-rich	proline, threonine, serine-rich
EukCats	novel voltage-gated Na^+- and Ca^{2+}-permeable channels
PDCs	putative cell-substratum adhesion molecules
CAMs	cell adhesion molecules
CLSM	confocal laser scanning microscopy
GlcA	glucuronic acid (GlcA)
Fuc	fucose (Fuc)
FGGs	highly sulfated fucoglucuronogalactans (FGGs)
ConA	Concanavalin A lectin
PSA	*Pisum sativum* lectin
LEA	*Lycopersicon esculentum* lectin

1 Motility

Diatom motility is characterized by a relatively smooth gliding motion that only occurs when cells are in contact with a surface (Sup Movie 1). It does not require any changes in cell shape or the movement of extended cellular extensions such as flagella or cilia that are utilized by many free-swimming organisms. Although active motility has been observed in a few araphid pennate species (e.g. *Licmophora hyaline*, Sato and Medlin 2006) and the pennate-like centric diatoms *Ardissonea crystallina* (Pickett-Heaps et al. 1991) and *Toxarium undulatum* (Kooistra et al. 2003), it is largely restricted to raphid pennate species that possess a specialized slit in their silica cell wall termed the raphe (Fig. 1). In motile araphid species, it is thought that mucilage secreted from a pore at one end of the cell swells and pushes the cell forward (Pickett-Heaps et al. 1991; Sato and Medlin 2006), whereas in raphid species, the secretion of mucilage can take place along the entire raphe slit.

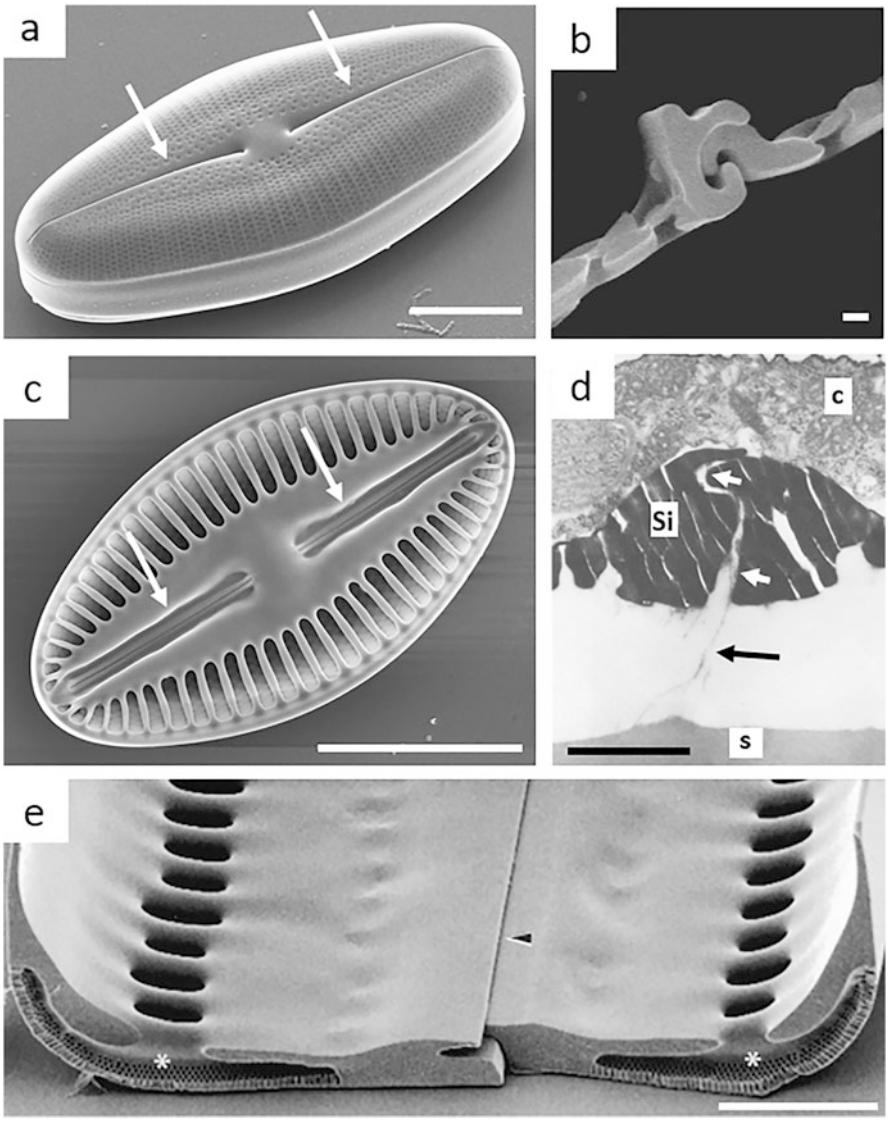

Fig. 1 (**a**, **c**) Mature valve morphology of *Diploneis smithii*, white arrows show position of the raphe slits. Scale bar: 10 μm (Idei et al. 2018, *reprinted with permisssion from the Journal of Phycology*). (**a**) external valve surface (**c**) internal valve surface (**b**) Cross-section at the valve centre of *Navicula ramosissima* showing details of the C-shaped raphe fissure. Scale bar: 100 nm (Massé et al. 2001, *reprinted with permisssion from the Journal of Microscopy*). (**d**) TEM cross-section of a *Navicula cuspidata* raphe (white arrows), showing the adhesive strands (black arrow) extending from the raphe, *s* substratum, *Si* silica cell wall, *c* cytoplasm. Scale bar: 1 μm (Edgar 1983, *reprinted with permisssion from Protoplasma*). (**e**) SEM cross-section of *Pinnularia viridis* frustule cleaved by mild sonication. Arrow shows the raphe slits, asterisks show foramen chamber. Scale bar: 5 μm (Crawford et al. 2001, *reprinted with permisssion from the Journal of Phycology*)

The raphe is typically composed of two longitudinal slits in the hardened cell wall that are positioned end-to-end along the midline of each valve and are separated by a silica bridge termed the central nodule (Fig. 1a, c). There are a wide variety of raphe shapes, but in general, they are all complex interlocking structures that mechanically stabilize the slotted valve against orthogonally applied forces (Fig. 1). While the raphe is unquestionably involved in cell motility, precisely, how mucilage is secreted and translocated through it, and how this enables cell motility, remains unknown.

Motile diatoms glide at remarkable velocities of up to 25 μm s^{-1} (Cohn and Disparti 1992; Edgar and Pickett-Heaps 1984), which exceed those of other substratum-mediated types of motility, such as the gliding of Apicomplexans (e.g. *Toxoplasma* parasites: 3–5 μm s^{-1}) (Herm-Götz et al. 2002) or slow-crawling locomotion (e.g. glioma cells: 0.01 μm s^{-1}; Amoeba *Dictyostelum discoideum*: 0.15 μm s^{-1}; fish kerocytes: 1 μm s^{-1}) (Handel 2017). Diatoms are able to exert a well-regulated control over their movement, in which the cells frequently change their directions in response to external stimuli (Cohn et al. 2003, 2016; Edgar 1979). The stop-start, jerky motion of diatoms as they rapidly accelerate and decelerate is due in part to their small cell size and their high density silicified cell wall, resulting in their associated very low Reynolds number (the ratio of inertia to viscosity of a fluid), which is in the region of 10^{-4} (Edgar 1982). Therefore, the inertial forces experienced by a diatom cell are extremely small and cells are not able to move in the absence of active force generation.

Currently, the most accepted theory for the generation of the force required for diatom gliding involves an actin-myosin system (Edgar and Pickett-Heaps 1984). The actin component is comprised of two distinct bundles that lie immediately proximal to the plasma membrane along and underneath each raphe (Fig. 2) (Edgar and Pickett-Heaps 1983; Edgar and Zavortink 1983). The roles of actin and myosin in diatom motility were supported by drug inhibition studies using the actin-disrupting agent latrunculin and the myosin inhibitor BDM, which both reversibly inhibited diatom motility (Poulsen et al. 1999). Already more than 35 years ago, Edgar and Pickett-heaps combined observations of particles streaming along the raphe (Fig. 2e, f) with the discovery of the raphe-associated actin bundles to suggest a model for diatom gliding that was inspired by other known cell motility systems at the time (Edgar and Pickett-Heaps 1984). This model suggests that there is a physical connection between adhesive mucilage secreted from the raphe and the intracellular actin bundles via a continuum of biomolecules that span the plasma membrane (Fig. 2c). A force that is applied parallel to the actin filaments would then result in movement of the cell in the opposite direction. Wetherbee and coworkers extended this model to include myosins, which are the only known motor proteins to generate force along actin cables. They termed the proposed continuum of biomolecules that includes the myosins, transmembrane proteins, and the adhesive mucilage the Adhesion Motility Complex (AMC) (Wetherbee et al. 1998). Genome sequencing has revealed that motile diatoms possess at least nine different myosins (Heintzelman and Enriquez 2010; Osuna-Cruz et al. 2020); however, it is not known which of these play a role in cell motility, and the existence of the AMC remains to be verified.

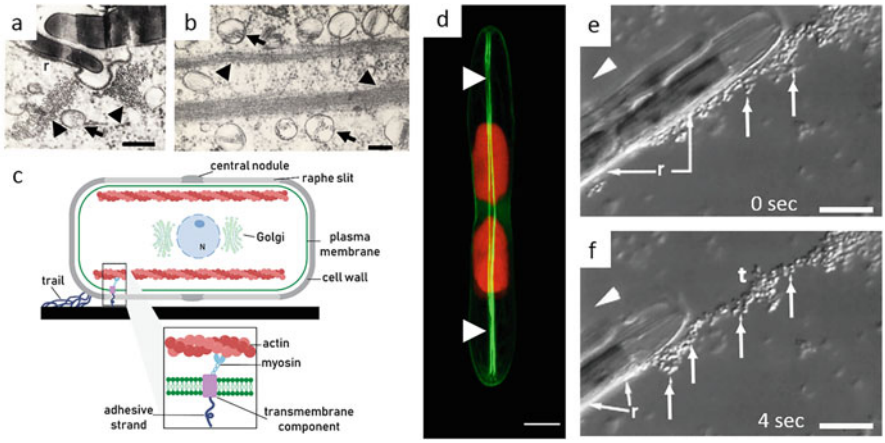

Fig. 2 (**a**, **b**) TEM cross-section of *N. cuspidata* showing details of the raphe (r) and associated actin filaments (arrow heads) and vesicles (arrows). Scale bars: 0.1 μm (Edgar and Pickett-Heaps 1983, *reprinted with permisssion from the Proceedings of the Royal Soceity B. Biological Sciences*). (**c**) Model for diatom gliding. Longitudinal section through a gliding diatom. The adhesive mucilage is processed and packaged into vesicles within the Golgi complex and transported to the plasma membrane. Once the vesicles are secreted, the adhesive mucilage forms strands that extend through the raphe slit attaching the cell to the substratum. At their proximal ends, the mucilage strands are linked via a continuum of molecules, including transmembrane proteins, to the myosin motor, which generates force along the underlying actin cytoskeleton. The rearward translocation of the adhesion complexes results in forward movement of the cell (adapted from Edgar and Pickett-Heaps 1984). *N* nucleus (**d**) Raphe-associated actin bundles (arrow heads) GFP-tagged with Lifeact (green) in *Craspedostauros australis* and chloroplast autofluorescence (red). Scale bar: 5 μm (Davutoglu & Poulsen, unpublished data). (**e**, **f**) Time lapse light microscopy of *C. australis* cells and silica microspheres. The cells were allowed to settle onto a glass slide, layered with a slurry of silica microspheres (0.6 μm diameter) and sequences of the cells interacting with the microspheres were recorded (E: 0 s; F: 4 s). The cell is attached to the substratum at the raphe (r) but has tilted slightly revealing the silica microspheres (small arrows) that have also adhered to the raphe and form a trail (t) behind the moving cell. The direction of cell movement is indicated by the large arrowhead. Scale bars: 10 μm (Lind et al. 1997, *reprinted with permission from Planta*)

An early explanation for diatom motility was jet propulsion, in which it was believed that the expulsion of fluid from the raphe or pores in the cell wall would drive locomotion (Lauterborn 1896). However, a key observation arguing against jet propulsion and supporting the existence of the AMC is the so-called streaming of particles along the raphe. For more than two centuries, it has repeatedly been shown that free-floating particles (e.g., soluble ink, silica beads) can attach to the raphe and be seen moving bidirectionally along the raphe in both stationary and gliding cells (Edgar and Pickett-Heaps 1984; Drum and Hopkins 1966; Harper 1967; Lind et al. 1997; Müller 1893) (Fig. 2e, f). In a jet propulsion mechanism, the beads would be expected to be pushed away from the raphe; therefore, this model for motility is no longer accepted. Interestingly, upon reaching the central nodule of the raphe, particles are capable of traversing this break and continuing to move as a single unit. Particles traveling along the dorsal (nondriving) raphe can be seen moving in

both directions, simultaneously along the same section of the raphe. Furthermore, they are capable of changing direction and their movement appears to be independent of the direction and velocity of cell gliding. In contrast, particles streaming along the ventral (driving) raphe always move in the opposite direction of cell movement, except for when a cell is in the process of reversing its direction (Edgar 1979; Edgar and Pickett-Heaps 1984). During a change in cell direction, particle streaming is reversed first in the rear half of the cell, upon which the cell pauses before changing direction, followed by a reversal in the direction of particle streaming on the other half of the raphe (Edgar and Pickett-Heaps 1984). Finally, when the direction of cell movement has been reversed, both ventral raphes stream in the opposite direction to cell movement, suggesting that a rearward translocation of the AMC drives forward movement of the cell. These observations clearly demonstrate the existence of a physical connection between the extracellular material that adheres to the particles and an intracellular bidirectional highway that controls their movement along the raphe slit. The fact that beads can move in a bidirectional manner along the dorsal, nondriving raphe, even when a cell is not moving, suggests that co-ordinated movement of the AMC is traction-force mediated.

Two alternate theories have been proposed to explain the mechanism of diatom motility. One was provided by Gordon and Drum, who proposed a "capillary model" where cell movement is driven by the energy derived from the hydration of the adhesive mucilage as it is secreted from the raphe slit, rather than the force generation coming from the internal cytoskeleton (Gordon 1987; Gordon and Drum 1970). To date, no further evidence has been provided to support this model. More recently, Wang and coworkers questioned whether the actin cables in the Edgar and Pickett-Heaps model are capable of acting as "intracellular railways" to support the high bidirectional speeds of diatom gliding (Wang et al. 2013). Instead, based on studies with a *Navicula* sp., they proposed that motility is generated via two or more plasma membrane invaginations (pseudopods) containing F-actin. In their model, the pseudopods would protrude through the raphe, generate friction, and propel the cell forward through their repeated attachment and detachment from the surface. However, the refractive structures, which are suggested to contain F-actin in this model, have previously been described as volutin granules in *Navicula* and *Sellaphora* species that contain inorganic polyphosphate (Mann 1985, 1989) and are not present in all motile species. Moreover, other than some observations of pits along the mucilage trails, there is no evidence of membranous cellular extensions projecting through the raphe. Therefore, further evidence is required to confirm the presence of F-actin in these structures and the extrusion of the pseudopods from the raphe slit. The claim by Wang and coworkers that myosins are unable to produce the force for the high motility speed of diatoms and their bidirectionality is not justified. In vitro assays have demonstrated that myosins are able to transport cargoes at speeds between 0.2 and 60 μm s^{-1} [e.g., myosins V (Pierobon et al. 2009), myosin II (Rastogi et al. 2016), myosins from the green alga *Chara* sp. (Higashi-Fujime et al. 1995)]. Bidirectionality of movement could be achieved through the involvement of the minus-end-directed myosin VI, which moves in the opposite direction to conventional myosins (Sweeney and Houdusse 2010). Additionally, the

F-actin bundles may be composed of filaments with opposite polarities, allowing myosin-based force generation in either direction along the raphe.

1.1 Regulation of Diatom Motility

1.1.1 Phototaxis

Diatom migration patterns are regulated by both endogenous (cell cycle, circadian rhythms) and exogenous (environmental conditions) factors and are largely a response of the cells' requirement for photosynthesis (Barnett et al. 2020; Cohn and Disparti 1994; Cohn et al. 1997, 2000, 2004; McLachlan et al. 2009; Perkins et al. 2010; Prins et al. 2020; Serôdio et al. 2008; Underwood et al. 2005). Benthic habitats are highly dynamic ecosystems that undergo rapid changes in environmental conditions. Tidal changes, wave action, sediment composition, shading, and water column turbidity all necessitate an active response of cells to maintain their position relative to incoming light. Observations of the color changes in intertidal sediments that contain diatom-rich biofilm communities demonstrate these predictable diurnal and tidal diatom migration patterns, which allow for light capture during the day and migration to nutrient-rich environments at night (Consalvey et al. 2004; Daglio et al. 2016; de Brouwer and Stal 2001; Ezequiel et al. 2015; Paterson 1986). The cell movement toward areas of moderate light intensity is the result of a photophobic response to find an ideal compromise between the need for photosynthesis (negative photophobic response; into-light movement) and the avoidance of high light intensity that causes oxidative damage to the photosystems (positive photophobic response; out-of-light movement) (Cohn and Weitzell 1996; Nultsch 1971; Nultsch and Häder 1988). Impressively, these vertical migration patterns are reset daily and fortnightly to match the tide timings and seasonal changes in day length (Barnett et al. 2020). Recently, a cleverly designed ex situ experimental setup has been used to monitor vertical migration dynamics using Chlorophyll *a* fluorescence coupled with imaging techniques (Imaging-PAM fluorometer) (Barnett et al. 2020). The migration rhythmicity was shown to be primarily coupled to the tidal, lunar cycle but can be further modulated by light (both light intensity and diurnal pattern), with a positive effect of blue wavelengths compared to other wavelengths (i.e., white, green, and red light) (Barnett et al. 2020).

Diatom phototactic responses are dependent on the wavelength of the light, with some species responding more strongly to blue-green light (450–500 nm), while others show a maximal response to red-orange light (~650 nm) (Cohn and Weitzell 1996; Cohn et al. 1999, 2015, 2016; Nultsch 1971). Species-specific responses to light have important ecological implications as they allow more diverse communities of diatoms to inhabit the same intertidal sediments. Competition due to their preference for different wavelengths and intensities results in species-specific diurnal migration patterns. The photophobic response of individual cells can also vary depending on the specific area of the cell that is exposed to high intensity light (i.e. "leading" vs. "trailing" end) with cells more responsive to light activation at the leading edge of the cell (Cohn et al. 1999, 2004; Nultsch 1971) (Fig. 3a). When the

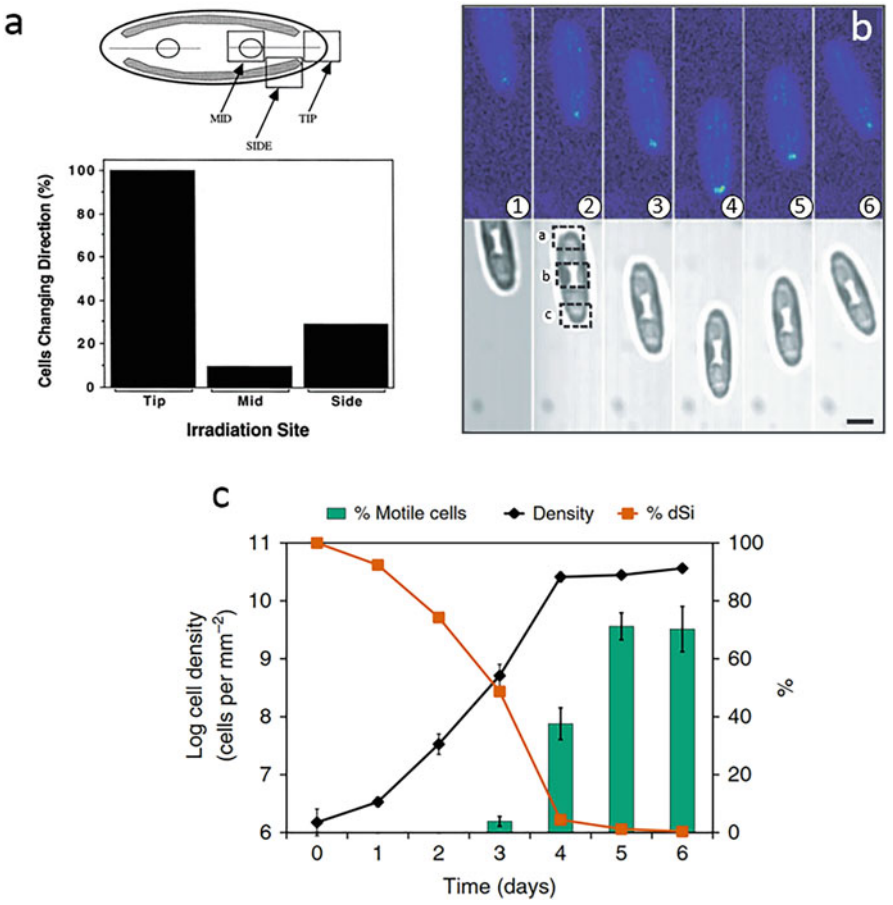

Fig. 3 (**a**, **b**) Photophobic response of *C. cuspidata* (**a**) *and N. perminuta* (**b**). (**a**) Individual cells were irradiated for 1 s with 545 nm light at different positions along the cell body. The percentage of cells changing direction after irradiation at the indicated sites is shown (Cohn et al. 1999, *reprinted with permission from Diatom Research*). (**b**) During the photophobic response, an increase in Calcium Crimson fluorescence was seen at the tip of the cell. Scale bar: 5 μm (McLachlan et al. 2012, *reprinted with permission from the Journal of Phycology*). (**c**) During growth of *S. robusta*, cell motility increased while dissolved Si (100% dSi = 106 μM) was being depleted and the culture entered stationary phase. Error bars show the standard error of the mean of five replicates ($n = 300$) (Bondoc et al. 2016a, *Creative Commons reprint permission*)

tip at the leading end of *Craticula cuspidata* was irradiated with blue light, all cells changed direction within 30 s, whereas irradiance at other parts of the cell resulted in a much lower response rate (10–30% of the cells) (Cohn et al. 1999) (Fig. 3a). Together these observations have led to the hypothesis that motile pennate diatoms regulate their motility by detecting boundaries of changes in light intensity (Cohn 2001), which might trigger a response in membrane-bound photoreceptors (e.g., second-messenger-dependent signal transduction cascades) that would elicit a

change in cell direction. An increase in the intracellular [Ca^{2+}] at the tips of the cells at the precise moment of cell direction change has been demonstrated using the fluorescent calcium indicator Calcium Crimson (Fig. 3b) (McLachlan et al. 2012). This result supports the hypothesis that chloroplast-independent photoreceptors are responsible for motility switching (McLachlan et al. 2012). Diatom genomes encode multiple candidates for photoreceptors that mediate photosynthesis-independent cellular responses to light (see chapter "Photosynthetic Light Reactions in Diatoms. I. The Lipids and Light-Harvesting Complexes of the Thylakoid Membrane"). However, until now it is unknown whether any of these photoreceptors are involved in phototaxis.

Although not as well studied as phototaxis (a directional response to light), diatoms also exhibit photokinesis, which is a change in cell speed as a response to light. Nultsch (1971) demonstrated that *Nitzschia communis* increases cell speed when it is transferred from dark to light conditions but that an increase in light intensity above 500 lux resulted in a decrease in speed. A similar trend was also observed for *Navicula perminuta* and *Cylindrotheca closterium*, and it was suggested that photokinesis contributes to efficient light-stimulated dispersal with red light producing the highest cell speeds (McLachlan et al. 2009).

1.1.2 Chemotaxis

The dominance of marine ecosystems by diatoms is hypothesized to be due to their ability to rapidly respond to changing environmental cues, such as nutrient supply (see chapters "Comparative and Functional Genomics of Macronutrient Utilization in Marine Diatoms" and "Molecular Mechanisms Underlying Micronutrient Utilization in Marine Diatoms"). However, little is known about the molecular underpinnings of these responses with respect to benthic diatom motility. *Amphora coffeaeformis* was shown to respond to various sugars, with D-mannose and L-glucose inducing a strong negative response, while D-glucose induced positive chemotaxis (Cooksey and Cooksey 1988). Cells adjusted their movement pattern to follow a concentration gradient, provided they were not previously exposed to a glucose-rich environment that apparently desensitized their ability to sense sugar molecules. The benthic diatoms *Seminavis robusta* and *Navicula* sp. increased EPS production and motility speed when silicic acid (dSi) or orthophosphate (dP) concentrations were depleted (Bondoc et al. 2016a, 2019) (Fig. 3c). When a localized dSi source was introduced into a dSi-starved culture, the cells moved faster and their foraging behavior was characterized by increased reversals and circular movement behaviors to optimize their search for the dSi source (Bondoc et al. 2016a, 2019).

Diatom gliding is also sensitive to external [Ca^{2+}], which may serve two independent functions. Firstly, an influx of Ca^{2+} may act as a second messenger for the secretion of EPS and/or the regulation of cytoskeleton dynamics (McLachlan et al. 2012). Secondly, functionality of the biopolymers of the secreted adhesive mucilage may require cross-linking via Ca^{2+}-ions (Chiovitti et al. 2008; Cooksey and Cooksey 1980). Although external calcium is important for gliding, it is not essential as decreasing the [Ca^{2+}] in the medium and application of a Ca^{2+} channel blocker

does not completely abolish cell movement and has no effect on the photophobic response (McLachlan et al. 2012). Inhibitors of Ca^{2+} homeostasis did not significantly reduce cell speed but caused a significant decrease in the photophobic response. Recently, a novel family of voltage-gated Na^{+}- and Ca^{2+}-permeable channels (EukCats) has been implicated in regulating internal calcium levels that are believed to be required for gliding motility (Helliwell et al. 2019). *Phaeodactylum tricornutum* cell lines in which the PtR1-eukcatA1 gene was knocked out using CRISPR/Cas9 exhibited reduced cell velocity compared to wild-type cells (Helliwell et al. 2019).

Sexual reproduction in raphid pennate diatoms requires active motility for the pairing of distinct mating types (MT+ and MT−) and relies on the production of both sex-inducing (SIPs) and attracting pheromones that activate mating behavior and guide the cells in their search for a mating partner (see chapter "Life-Cycle Regulation"). To date, the only characterized raphid diatom pheromone is diproline, which is released by *S. robusta* MT− cells in response to perceiving a chemical signal from MT+ cells. Using polymer beads loaded with diproline, MT− cells displayed increased cell motility with a preferred forward movement to the pheromone-loaded beads (Bondoc et al. 2016b; Gillard et al. 2013). Recently, the motility of *S. robusta* and *C. closterium* MT+ cells in response to the SIP produced by the MT− mating type (SIP-) was shown to increase the fraction of motile cells and the average motility speed (Bilcke et al. 2021; Klapper et al. 2021). However, the molecular composition of the SIP remains unknown.

Several other external environmental factors have been shown to influence diatom motility, such as temperature, salinity, gravity, surface chemistry, and pH. The optimal temperature, pH, and salinity are important parameters for motility, but are species-specific and depend largely on the environmental conditions in their local habitat to which they have acclimated (Apoya-Horton et al. 2006; Cohn and Disparti 1992; Cohn et al. 2003; Du et al. 2012; Gupta and Agrawal 2007; Hopkins 1963; Sauer et al. 2002). Interestingly, the type of movement displayed by the mudflat diatom, *C. closterium*, also alters according to the salinity conditions, with a reduction in gliding movement under hyposaline conditions (Apoya-Horton et al. 2006). The raphe in *C. closterium* follows a pronounced twist around the cell body and observations of its gliding behavior revealed that in addition to the smooth gliding common to other diatoms, they exhibit a "corkscrew" gliding motion with a rotation about the *x*-axis (Apoya-Horton et al. 2006). Together with gliding, pivoting and pirouetting cell movements were also observed and suggested to be a result of a sensory detection system in the cell tips that may respond to light and other environmental cues.

Recently, it has been demonstrated that benthic diatoms, in the absence of other external stimuli, are able to sense gravity and use it to orient themselves relative to the surface (Frankenbach et al. 2014). Surface chemistry and roughness of the substratum have been shown to affect the speed of cell movements (Hodson et al. 2012; Holland et al. 2004; Scardino et al. 2006). The fraction of motile cells in a culture is higher on hydrophilic compared to hydrophobic surfaces (Holland et al. 2004). However, further experimentation is required to determine the influence of

surface chemistry on diatom motility characteristics including speed distribution, trajectories, as well as frequencies of reversals and stoppages.

2 Adhesion

Although diatoms are unicellular, some species form colonies with cells linked together through interlocking silica structures (see chapter "Structure and Morphogenesis of the Frustule") and/or extracellular polymeric substances (EPS). In some cases, mucilaginous EPS is produced along the whole valve face (e.g., *Fragilariopsis* sp.), which allows the cells to form long chains, whereas other species secrete EPS through specialized pores at the poles of the valve (e.g., *Thalassionema* sp.). These types of diatom adhesive structures are poorly characterized, and therefore, the remaining sections of this chapter will summarize the current knowledge on the composition and properties of diatom adhesives that are required for (1) motility (2) biofilm formation, and (3) sessile attachment.

2.1 Adhesives: Motility

The attachment and subsequent motility of raphid diatoms are reliant on the secretion of adhesive material that provides traction for (1) reorientation of cells to form raphe/substratum contacts and (2) directed motility. The adhesive material is believed to be produced in the Golgi apparatus and then packaged into vesicles. In electron microscopy studies, numerous vesicles containing "fibrillar" material have been found in close proximity to the raphe-associated actin bundles and scattered beneath the plasma membrane (Fig. 2) (Edgar and Pickett-Heaps 1982, 1983). However, conclusive evidence that these vesicles are derived from the Golgi apparatus and discharged their content into the raphe slit is still lacking. To investigate the structure of the adhesive material, electron microscopy (EM) and atomic force microscopy (AFM) techniques have been applied; yet, both techniques have severe limitations. The previously applied EM techniques introduced artifacts caused by the dehydration of the material and in some cases also by the use of chemical fixation methods. Using AFM, it was possible to image the adhesive material under hydrated conditions; yet, adhesion of the material to the cantilever tip substantially compromised the spatial resolution of the imaging procedure. The following two paragraphs summarize the main results that have been obtained from EM and AFM imaging of adhesive material.

Direct observations of the driving raphe are challenging as the EPS is damaged in the process of inverting the cell. Nevertheless, scanning EM (SEM) imaging has revealed the presence of mucilage strands along the entire length of the raphe slit (Edgar 1983; Higgins et al. 2003a; Webster et al. 1985) (Fig. 4a). Transmission EM (TEM) observations of *N. cuspidata* cells demonstrated that raphe-associated, bristle-like strands were found in a perpendicular orientation to the plasma membrane and not parallel as was previously suggested (Harper and Harper 1967) (Fig. 4d).

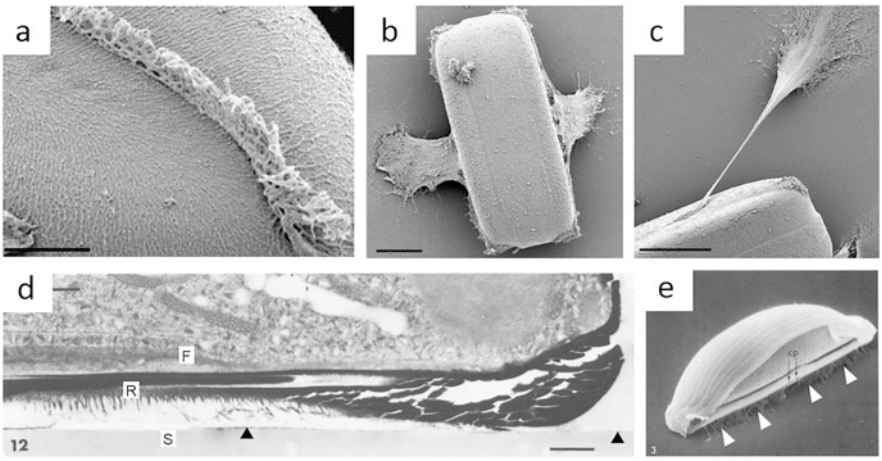

Fig. 4 (**a**–**c**) SEM of chemically fixed *P. viridis* cells (Higgins et al. 2003a, *reprinted with permission from the Journal of Phycology*). (**a**) Mucilage strands projecting from the raphe slit. Scale bar: 3 μm (**b**) A recently settled cell lands on its girdle bands and extends two sheets of mucilage from the midpoint of each valve surface to form a connection with the substratum. Scale bar: 15 μm. (**c**) A long thin strand of mucilage extending from the raphe slit and forming a holdfast-like attachment to the substratum. Scale bar: 15 μm. (**d**) TEM longitudinal section through the raphe slit of *N. cuspidata*. Mucilage strands project through the raphe slit (R) and attach the cell to the substratum (s), a layer of mucilage (arrowheads) coats the substratum. Scale bar: 1 μm (Edgar 1983, *reprinted with permisssion from Protoplasma*). (**e**) SEM of *Amphora* sp. showing mucilage strands (arrowheads) attaching the cell to the substratum, *cp* central pores of the raphe. Scale bar: 1 μm (Webster et al. 1985, *reprinted with permission from Cytoskeleton*)

Thick sheets (~15 μm) of intertwined strands emanating from the raphe slit have been observed in *Craspedostauros australis* and *Pinnularia* sp. and are proposed to be tethers involved in initial cell adhesion and reorientation (Higgins et al. 2003a) (Fig. 4b, c). When adhesive strands from both raphes engage with the surface, it is believed that there is a competing tension that results in a "tug of war" between the raphe systems on each valve. This leads to a rocking motion of the cell that is eventually broken as the force exerted by one raphe system exceeds that of the other and the cell is able to reorient, generate a connection with the "successful" raphe and commence gliding (Wetherbee et al. 1998).

In situ atomic force microscopy (AFM) revealed that there are at least two different types of secreted material associated with the diatom cell wall: (1) a soft, weakly adhesive cell coating and (2) an adhesive material that is projecting from the raphe slit (Arce et al. 2004; Chiovitti et al. 2006; Dugdale et al. 2005a, b, 2006a, b; Gebeshuber et al. 2000, 2002, 2003; Higgins et al. 2003a, b). The cell coating is composed of a soft mucilage (10–25 nm thick) that differs significantly in morphology between different species (Fig. 5a–c) (Gebeshuber et al. 2000; Higgins et al. 2003b). The cell surface of *C. australis* is covered in a relatively smooth layer of mucilage, a *Pinnularia* sp. is covered in mucilaginous spheres and while most of the

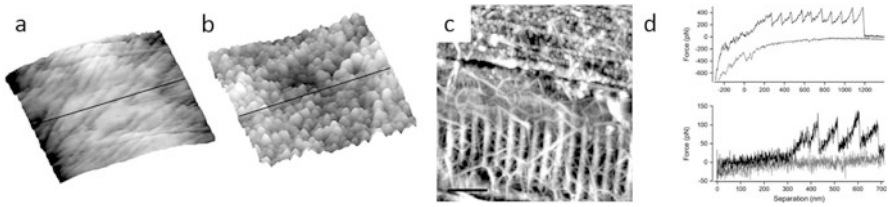

Fig. 5 AFM imaging and force spectroscopy. (**a–c**) Tapping mode height images of the mucilage cell coating from (**a**) *C. australis.* Scale bar: 2.5 μm (**b**) *P. viridis*. Scale bar: 2.5 μm and (**c**) *Nitzschia navis-varingica.* Scale bar: 1 μm (Higgins et al. 2003b, *reprinted with permission from the Journal of Phycology*). (**d**) Force versus separation curves recorded from the surface of stationary ovoid *P. tricornutum* cells representing adhesive nanofibers (*top*) and a single modular protein (*bottom*) (Dugdale et al. 2006b, *reprinted with permission from the Biophysical Journal*)

Nitzschia navis-varingica cell wall is not covered in mucilage, some regions are covered in a network of long strands (Fig. 5a–c) (Higgins et al. 2003b). Until now, direct AFM imaging of the raphe adhesive strands has not been possible due to their high mobility and strong adhesion to the cantilever tips. AFM force curve measurements of raphe secreted mucilage strands revealed self-healing properties and higher detachment forces compared to the cell coating (e.g., for *C. australis*: Fmax = 3.2 ± 1.9 nN vs 0.2 ± 9E-03 nN) (Chiovitti et al. 2006; Dugdale et al. 2006a, b; Higgins et al. 2003a). When the AFM cantilever tip was brought into contact with the raphe-associated mucilage strands and then retracted until the force caused the strands to detach, multiple peaks in the force-distance plot were observed ("sawtooth pattern"; Fig. 5d). The sawtooth pattern was interpreted as the unfolding of adhesive domains or breakage of sacrificial bonds within or between the mucilage strands (Gebeshuber et al. 2002; Higgins et al. 2003a; Molino et al. 2006). Utilizing a "fly-fishing" technique, where the AFM cantilever tip is hovered above the diatoms cell surface until an interaction with the most protruding strand is recorded, has enabled measurement of the physical properties of individual *P. tricornutum* adhesive strands. From the obtained data, it was suggested that individual adhesive strands are composed of modular proteins with domains of 336 amino acids that unfold successively as the cantilever tip is retracted (Dugdale et al. 2006b).

2.2 Diatom Trails

As diatom cells glide across a substratum, they deposit behind them mucilage secretions, termed "diatom trails." The trails are believed to be the remnants of the adhesive material that provides the traction for cell movement that have been shed from the distal end of a moving cell. These trails have first been visualized indirectly using light microscopy by the adsorption of particles (e.g., charcoal, silica, or polystyrene microbeads) and various more or less specific histochemical stains. The latter indicated the presence of polyanionic compounds, such as carbohydrates and proteins (Daniel et al. 1987; Molino and Wetherbee 2008; Poulsen et al. 2014;

Wigglesworth-Cooksey and Cooksey 2005) (Fig. 6). More recently, diatom trails have been imaged directly by AFM, which is challenging as the material is extremely soft, strongly adhesive, and is easily dislocated as it sticks to the cantilever tip upon contact, thereby leading to imaging artifacts. Native hydrated adhesive material deposited by a *Pinnularia* sp. was imaged using contact and fluid tapping modes, revealing the presence of trails with a width of 2–3 µm, which formed continuous, swollen rounded structures up to 300 nm high that smeared during imaging (Higgins et al. 2000). After dehydration the trails could be easily visualized (Chen et al. 2019) (Fig. 6a); however, they are greatly reduced in width (1–1.5 µm) (Higgins et al. 2000), which highlights the importance of imaging diatom EPS structures in their native, hydrated form.

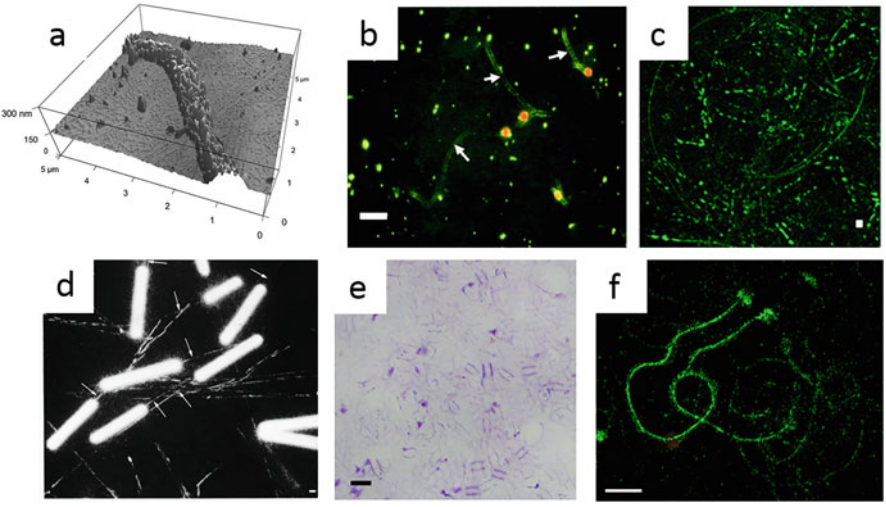

Fig. 6 (**a**) AFM 3D topography image of a dehydrated trail from *Navicula* sp. (Chen et al. 2019, *reprinted with Creative Commons license permission*). (**b**) Diatom trails (arrows) from *A. coffeaeformis* stained with FITC-concanavalin A. Scale bar: 50 µm (Wigglesworth-Cooksey and Cooksey 2005, *reprinted with permission from Applied Environmenal Microbiology*). (**c**) *C. australis* stained with the fucose-specific lectin AAL-FITC. Scale bar: 10 µm (Neu and Kuhlicke 2017, *reprinted with Creative Commons license permission*). (**d**) Immunofluorescence labeling of *C. australis* trails (arrows) with the monoclonal antibody StF.H4. Scale bar: 20 µm (Lind et al. 1997, *reprinted with permission from Planta*). (**e**) *A. coffeaeformis* trails stained with the dye Stains All. Scale bar: 20 µm. (Poulsen, unpublished) (**f**) *A. coffeaeformis* trail labelled with anti-Ac629 antibodies. Scale bar: 10 µm (Lachnit et al. 2019, *reprinted with permission from the Philosophical Royal Society B Biological Sciences*)

2.3 Molecular Composition of Diatom Adhesives Involved in Cell Motility

The biochemical isolation and characterization of the diatom adhesives is very challenging as they are very sticky and difficult to separate from the intact cells. Therefore, many studies have used indirect observations (e.g., lectin and chemical staining) and although the precise molecular composition of the adhesives involved in diatom motility remains to be determined, evidence suggests that they are largely composed of complex, anionic polysaccharides and a smaller amount of protein (Bahulikar and Kroth 2007; Chiovitti et al. 2003, 2008; Daniel et al. 1980, 1987; Lachnit et al. 2019; Lewin 1958; Lind et al. 1997; Poulsen et al. 2014; Willis et al. 2014; Wustman et al. 1997, 1998) (Fig. 6). The monosaccharide composition has been investigated using fluorescently tagged lectins, which are carbohydrate-binding proteins highly specific for certain types of sugars. Using a library of 88 lectins, it was revealed that the fucose-binding lectin AAL recognizes trails secreted by all seven diatoms tested and the β-N-acetyl glucosamine–binding lectin, LEA recognized material from six of the seven species (Neu and Kuhlicke 2017). For 44 of the other 86 lectins, the trails of each species displayed different recognition patterns, suggesting that there is a wide variety in the composition of diatom EPS. However, some caution must be taken when analyzing these results as the experimental setup and processing can influence the specificity of the lectin binding. For example, in one study, the diatom *A. coffeaeformis* tested negative for concanavalin A (binds to α-glucose, α-mannose, and α-N-acetyl glucosamine) (Neu and Kuhlicke 2017) and positive in another (Wigglesworth-Cooksey and Cooksey 2005). Immunofluorescence studies using monoclonal antibodies raised against cell wall–associated glycoproteins from *C. australis* labeled both the cell walls and trails deposited by moving cells (Fig. 6d) (Lind et al. 1997). Subsequent studies revealed that these antibodies were specific to the carbohydrate moieties rather than the protein backbone (Chiovitti et al. 2003). The chemical structure of the carbohydrate epitope recognized by the monoclonal antibodies remains unknown.

Recently, a method was developed that allowed for the isolation of the diatom trail material, and biochemical analysis of the trails from *A. coffeaeformis* and *C. australis* that revealed the predominance of carbohydrates (~70%) over proteins (~30%) (Poulsen et al. 2014). The carbohydrates were dominated by uronic acids and the proteins by hydrophilic amino acids including the rare 2,3-*cis*-3,4-*trans*-dihydroxy-L-proline. This analysis provided the first direct evidence of proteins in the adhesive trails (Poulsen et al. 2014). A subsequent proteomics analysis of the adhesive trails from *A. coffeaeformis* identified 21 proteins of which 13 are diatom-specific proteins of unknown function and the remaining eight proteins share features with adhesive proteins in other organisms (i.e., fasciclin, choice-of-anchor A, PTS-rich, von Willebrand-D). Immunolocalization of some of these proteins has confirmed their presence in the adhesive trails, but their function in cell adhesion and/or motility is not yet known (Fig. 6f) (Lachnit et al. 2019). In *P. tricornutum*, ten putative cell-substratum adhesion molecules (PDCs) were identified using a bioinformatics screen based on the similarity of their

amino-acid composition to known cell adhesion molecules (CAMs) rather than sequence homology (Willis et al. 2014). Transgenic cell lines overexpressing three of the PDCs as GFP-tagged fusions proteins displayed increased cell adhesion to glass and increased adhesion events when the cells were probed using the AFM, suggesting that these proteins play a role in cell adhesion. None of these proteins have been localized at the raphe or the adhesive trails, and thus, it is still unclear whether they play a direct or indirect role in cell adhesion.

2.4 Biofilm Formation

In sunlit habitats, microbial biofilms are rapidly formed on submerged biotic and abiotic surfaces. Such biofilms are greenish-brown mucous layers composed of mixed microbiota communities dominated by bacteria, diatoms, fungi, unicellular algae, and protozoa (Fig. 7). The unique spectral emission signatures for different algal groups (i.e., cyanobacteria, green algae, and diatoms) allow for the specific mapping of species within the 3D biofilm community (Larson and Passy 2005) (Fig. 7c). In situ confocal laser scanning microscopy (CLSM) combined with microfluidic flow-cells systems for real-time imaging over extended durations has revealed the dynamics and growth of diatom biofilms (Bellinger et al. 2005; Larson and Passy 2005; Le Norcy et al. 2019; Rogers et al. 2010) (Fig. 7e–h). The biofilm communities reside within a 3D mucilaginous matrix of EPS that provides protection against environmental stresses (e.g., changes in temperature, pH, and salinity) and predators but also allows for nutrient sequestration and cell-cell communication (Molino and Wetherbee 2008; Stal 2010; Underwood 2010). A high production of biofilm EPS correlates with exposure to sunlight, nutrient limitation, and when cells transition from exponential growth into stationary phase (McConville et al. 1999; Smith and Underwood 1998; Staats et al. 2000a, b; Underwood 2010). Intertidal biofilm communities have many beneficial ecological roles. They stabilize benthic habitats by consolidating soft sediments, thus preventing erosion; they are an important carbon source for benthic organisms and are involved in nutrient cycling (de Brouwer et al. 2005; Kriwy and Uthicke 2011; Moss et al. 2006; Stal 2010). On the other hand, their attachment to man-made surfaces poses significant problems to maritime transport, aquaculture, and other aquatic industries. The formation of thick biofilm slimes on ship hulls increases frictional drag and fuel consumption by up to 18%, resulting in substantial worldwide economic losses (Schultz et al. 2011). Since the global ban on toxic antifouling coatings (e.g., tributyltin), there has been a demand to develop environmentally friendly, advanced antifouling surfaces to prevent the accumulation of microbial mass (Callow and Callow 2011).

Biofilm EPS is composed of up to 90% of polysaccharides, with the remainder being (glyco)proteins, nucleic acids, and lipids (Hoagland et al. 1993; Underwood 2010; Villacorte et al. 2015) (Fig. 7d). Determining the precise molecular composition of biofilms is extremely difficult as it is experimentally challenging to separate the gelatinous EPS matrix from intact cells. This has sometimes led to the incorrect assignment of intracellular components to the EPS (Chiovitti et al. 2004). In situ

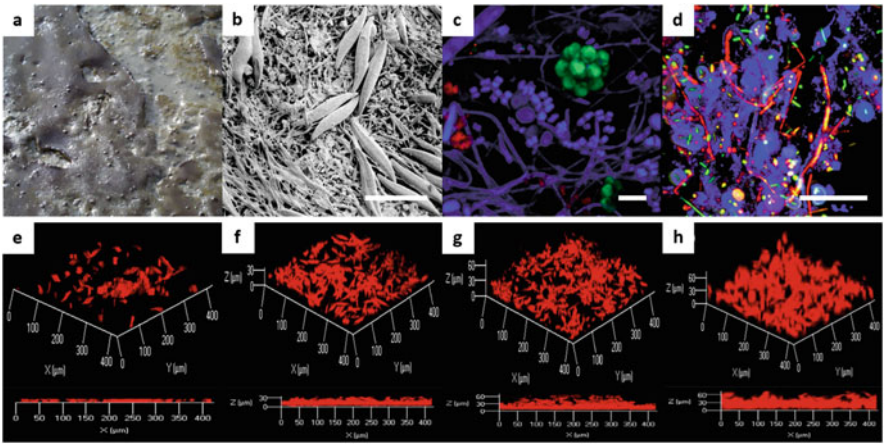

Fig. 7 (**a**) Diatom biofilm on muddy intertidal sediment of the Westerscheldt (Netherlands) (Stal 2010, *reprinted with permission from Ecological Engineering*). (**b**) Surface view of a species-rich biofilm dominated by *Pleurosigma* and *Gyrosigma* visualized by LTSEM. Scale bar: 100 μm (Underwood et al. 2005, *reprinted with permission from Limnology and Oceanography*). (**c**) CLSM image of a mixed community obtained by spectral separation and 3D reconstruction. Cyanobacteria (blue), green algae (green), and diatoms (red). Scale bar: 20 μm (Larson and Passy 2005, *reprinted with permission from the Journal of Phycology*). (**d**) Triple-labeled confocal images of different biofilms showing the distribution of nucleic acids (green), lipids (red), and polysaccharides (blue) labeled with N-acetylglucosamine- and N-acetyllactosamine-sensitive lectins. Scale bar: 10 μm (Lawrence et al. 2003, *reprinted with permission from Applied Environmental Microbiology*). (**e**–**h**) CLSM imaging of biofilm formation by *C. closterium* imaged by capturing the natural autofluorescence of chlorophyll ($\lambda_{excitation} = 633$ nm, $\lambda_{emission} = 638$–720 nm) (**e**) 48 h, (**f**) 72 h, (**g**) 96 h, (**h**) 120 h (Le Norcy et al. 2019, *reprinted with permission from International Biodeterioration and Biodegradation*)

approaches using fluorescently labeled lectins revealed the distribution of some specific glycoconjugates within the biofilm matrix (Fig. 7d) (Bahulikar and Kroth 2007; Neu and Kuhlicke 2017; Stal 2010; Wigglesworth-Cooksey and Cooksey 2005; Willis et al. 2013). Studies on the composition of biofilm EPS generally distinguish between three different fractions: (1) soluble, colloidal EPS, (2) loosely bound EPS, and (3) cell-bound EPS (de Brouwer and Stal 2002; Underwood 2010). The "soluble, colloidal fraction" is composed of mono-, oligo-, and polysaccharides (Underwood 2010). Monosaccharide analysis of the fractionated soluble biofilm EPS revealed that it contains high amounts of sulfate, uronic acids, and numerous other species-specific sugars such as galactose, fucose, mannose, xylose, and rhamnose (de Brouwer and Stal 2002; McConville et al. 1999; Staats et al. 1999; Underwood et al. 2004). The loosely and tightly cell-bound EPS are also dominated by the presence of complex carbohydrates (de Brouwer and Stal 2002; Staats et al. 2000b; Underwood 2010). However, care must be taken with the assignment of these fractions to the biofilm EPS as the techniques used may also extract intracellular components and cell-wall-associated material that are not components of the biofilm EPS (Chiovitti et al. 2004; Underwood 2010). Until now, the identity of

biofilm-specific proteins remains unknown. However, it seems possible that the adhesive trail proteins recently described from *A. coffeaeformis* may also play a role in biofilm formation (Lachnit et al. 2019).

Polar sea ice covers up to 13% of the world's surface and is a highly productive ecosystem, with an algal community dominated by diatoms thriving at the ice/water interface. EPS production by these psychrophilic diatoms alters the sea ice morphology and is thought to help the diatoms survive in these harsh conditions, which can drop below temperatures of −20 °C and reach a salinity above 20% (Underwood et al. 2010). *Fragilariopsis cylindrus* is prominently associated with Antarctic sea ice and is a model diatom species for studying their adaptation and response to this cold environment (Mock et al. 2017). Recently, the structural complexity of the *F. cylindrus* EPS was shown to increase at lower temperatures and higher salinities, which is believed to allow them to survive in their highly variable and extreme environment and has been linked to a reprogramming of the metabolic pathways involved in EPS production (Aslam et al. 2018).

To understand the interactions between diatoms and bacteria within a biofilm, mono- and multispecies biofilms have been cultured. This revealed that some species are able to coexist, whereas others can prevent biofilm formation, suggesting that there is competition and niche differentiation between some species (Buhmann et al. 2016; Doiron et al. 2012; Koedooder et al. 2019; Windler et al. 2015). For example, while some bacterial species produce vitamins beneficial for auxotrophic diatoms, others produce algicidal metabolites that induce diatom cell lysis (Croft et al. 2005; Paul and Pohnert 2011). A pronounced impact of bacteria on the biofilm-forming diatom *Achnanthidium minutissimum* was the production of an extracellular capsule that increased cell aggregation and attachment, whereas axenic diatom cultures grow in suspension (Windler et al. 2015).

2.5 Sessile Attachment

Some diatoms are capable of sessile adhesion, wherein the cell will attach permanently to a single position through the formation of adhesive pads, tubes, and stalks (Fig. 8) (Hoagland et al. 1993; Wang et al. 1997). Depending on the species and whether they are raphid, araphid, or centric diatoms, these adhesives structures are secreted from different cell wall structures such as the raphe, mantle edges, or pores in the apical end of the cell wall (Hoagland et al. 1993). Relative to motile cells, sessile diatoms are generally more strongly and flexibly attached to their substratum and are less likely to be detached by physical disruptions such as water currents.

The best studied sessile adhesive materials are the stalks produced by the raphid diatom *Achnanthes longipes*, which is capable of active motility but often transitions to a sessile lifestyle. Stalk formation is believed to be triggered by overcrowding due to high cell density, because it enables the cells to rise above the underlying biofilm (Fig. 8) (Wang et al. 1997, 2000). The stalks are organized into three distinct regions that differ both in structure and composition (1) a surface attached pad, (2) a collar linked to the frustule via a terminal nodule or apical pore, and (3) a shaft between the

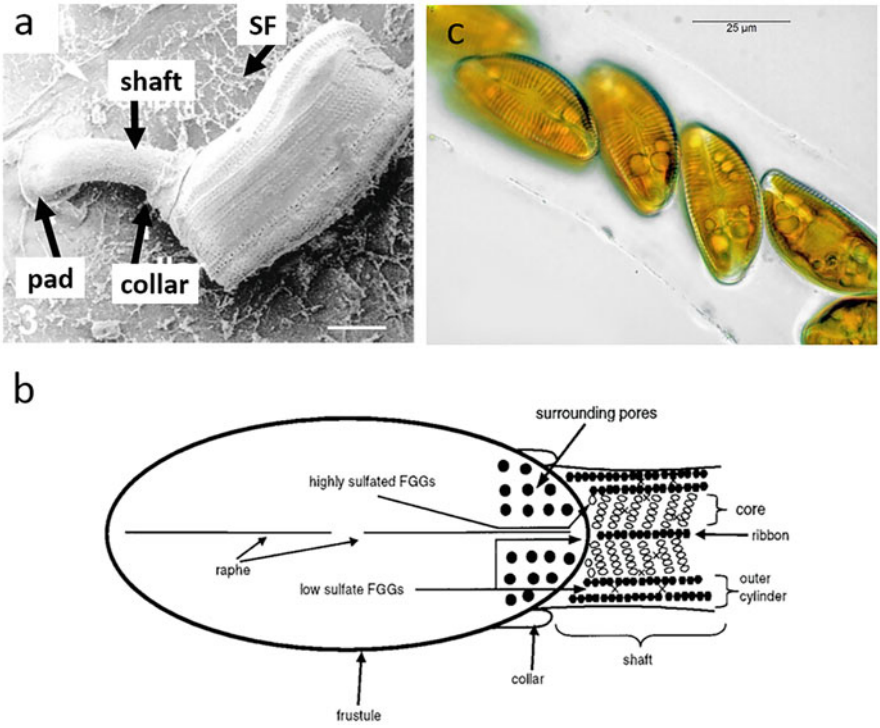

Fig. 8 *A. longipes* sessile adhesives (**a**) Cryo-SEM of the stalk composed of collar, shaft, and pad. Scale bar: 10 µm (Wang et al. 2000, *reprinted with permission from the Journal of Phycology*). (**b**) Model of the multilayer shaft composition (Wustman et al. 1998, *reprinted with permission from Plant Physiology*). (**c**) A colony of *Encyonema* sp. cells residing within a tube structure (image courtesy of Chris Carter)

cell and substratum (Daniel et al. 1987; Wang et al. 1997, 2000). The shaft of the stalk has a multilayer structure with a central ribbon of densely packed fibers, a surrounding diffuse layer, and an outermost layer. It was suggested that the central core region of the stalk is related to the adhesive used for cell motility and is secreted from the apical pore (Wustman et al. 1998). The autofluorescence of the stalks under UV light (>360 nm) suggests that the polymers are cross-linked by phenolic compounds (e.g., dityrosine, ferulic acid) (Wustman et al. 1997). Monosaccharide analysis and lectin labeling indicate that all regions of the stalk are composed largely of carbohydrates with a small amount of proteins. The adhesive pad contains substantial amounts of glucuronic acid (GlcA) and fucose (Fuc), the outer layer contains GlcA, Fuc and Galactose, and the inner core contains highly sulfated fucoglucuronogalactans (FGGs) (Wang et al. 1997; Wustman et al. 1998).

The benthic centric diatom *Toxarium undulatum* adheres to surfaces via secretion of an adhesive pad from their valve poles that is composed of protein, carbohydrate, sulfate, calcium, and magnesium (Chiovitti et al. 2008; Dugdale et al. 2006a). The

Ca^{2+} and Mg^{2+} ions are believed to be important for noncovalent cross-linking of the constituent biopolymers, because EDTA treatment resulted in a lack of the typical sawtooth pattern observed in the AFM force curves prior to EDTA treatment (Chiovitti et al. 2008; Dugdale et al. 2006a). Monosaccharide analysis of the adhesive pads revealed the presence of eleven neutral sugars with mannose and xylose, accounting for 79 mol%. EDTA extraction of the adhesive pads released an anionic high-molecular-weight (glyco) protein (>220 kDa). However, until now, the sequence of this protein remains unknown.

A very curious form of sessile diatom adhesion is the production of a hollow tube structure, within which colonies of motile cells reside (Houpt 1994) (Fig. 8c). These tubes can be several centimeters long and are composed predominantly of mucopolysaccharides (Bahulikar and Kroth 2007; Drum 1969; Lewin 1958). The tubes of *Cymbella caespitosa* were stained by the lectins ConA and PSA, indicating the presence of mannose and glucose moieties (Bahulikar and Kroth 2007). Tube formation is initiated by a single cell through the secretion of mucus from pores in the girdle band. Vegetative reproduction of the cell takes place once the tube reaches a length several times longer than the cell, and this results in the tube gradually filling up with cells that are able to move back and forth within the tube.

The invasive colonial freshwater diatom *Didymosphenia,* commonly known as rock snot*,* produces massive amounts of thick mats that are able to cover an entire river bed with a thickness greater than 20 cm (Spaulding and Elwell 2007). Even though the diatoms themselves are not considered harmful, these mats can cause a considerable negative impact on human activities as a result of their alteration of the natural ecosystem and the ability to alter the food web (Spaulding and Elwell 2007). It is not the cells themselves that cause the nuisance, but rather their massive production of extracellular stalks. These mats are largely composed of extracellular sulfated polysaccharide filaments and a smaller amount of proteins (Figueroa et al. 2020; Gretz 2008; Whitton et al. 2009).

3 Conclusion

For more than 200 years, diatom adhesion and motility has fascinated biologists and while some clues to the molecular mechanism have been gained, there are still many unanswered questions. Even today, there still exists a number of different hypotheses to explain this unique mode of cell motility (Edgar and Pickett-Heaps 1984; Gordon 1987; Wang et al. 2013). The most accepted hypothesis by Edgar and Pickett-Heaps, which argues for an adhesion/motility complex composed of a continuum of biomolecules spanning from the raphe-associated actin cables to the adhesive molecules, is still lacking direct confirmation. Future molecular and functional genetic studies are necessary to answer these questions, which will require the development of model systems to study diatom motility and adhesion. Although *P. tricornutum* has for many years served as a model pennate diatom for molecular research, it is not the most suitable species for studies on diatom motility as cells exhibit rather low motility and often only a small percentage of cells within a

population are motile as they switch between planktonic and benthic morphotypes. Therefore, recent and upcoming genome and transcriptome sequencing projects will inevitably expand the number of raphid pennate species that are suitable for molecular genetic studies and shed light on the molecular mechanism of motility.

Acknowledgments We are very grateful to the comments of the reviewers (Stanley Cohn, Graham Underwood, and Wim Vyverman) that have improved this book chapter. We would also like to thank Chris Carter for providing the image of the tube diatoms. This work was supported by the Deutsche Forschungsgemeinschaft (PO 2256/1-1).

References

Apoya-Horton MD, Yin L, Underwood GJ, Gretz MR (2006) Movement modalities as adaptive response to salinity changes of the mudflat diatom *Cylindrotheca closterium* (Bacillariophyceae). J Phycol 42:34–35

Arce FT, Avci R, Beech IB, Cooksey KE, Wigglesworth-Cooksey B (2004) A live bioprobe for studying diatom-surface interactions. Biophys J 87:4284–4297

Aslam SN, Strauss J, Thomas DN, Mock T, Underwood GJC (2018) Identifying metabolic pathways for production of extracellular polymeric substances by the diatom *Fragilariopsis cylindrus* inhabiting sea ice. ISME J 12:1237–1251

Bahulikar RA, Kroth PG (2007) Localization of EPS components secreted by freshwater diatoms using differential staining with fluorophore-conjugated lectins and other fluorochromes. Eur J Phycol 42:199–208

Barnett A, Méléder V, Dupuy C, Lavaud J (2020) The vertical migratory rhythm of intertidal microphytobenthos in sediment depends on the light photoperiod, intensity, and spectrum: evidence for a positive effect of blue wavelengths. Front Mar Sci 7:212

Bellinger BJ, Abdullahi AS, Gretz MR, Underwood GJC (2005) Biofilm polymers: relationship between carbohydrate biopolymers from estuarine mudflats and unialgal cultures of benthic diatoms. Aquat Microb Ecol 38:169–180

Bilcke G, Van den Berge K, De Decker S, Bonneure E, Poulsen N, Bulkankova P, Osuna-cruz CM, Dickenson J, Sabbe K, Pohnert G, Vandepoele K, Mangelinckx S, Clement L, De Veylder L, Vyverman W (2021) Mating type specific transcriptomic response to sex inducing pheromone in the pennate diatom *Seminavis robusta*. ISME J 15:562–576

Bondoc KGV, Heuschele J, Gillard J, Vyverman W, Pohnert G (2016a) Selective silicate-directed motility in diatoms. Nat Commun 7:10540

Bondoc KGV, Lembke C, Vyverman W, Pohnert G (2016b) Searching for a mate: pheromone-directed movement of the benthic diatom *Seminavis robusta*. Microb Ecol 72:287–294

Bondoc KGV, Lembke C, Vyverman W, Pohnert G (2019) Selective chemoattraction of the benthic diatom *Seminavis robusta* to phosphate but not to inorganic nitrogen sources contributes to biofilm structuring. Microbiology 8:e694

Buhmann MT, Schulze B, Förderer A, Schleheck D, Kroth PG (2016) Bacteria may induce the secretion of mucin-like proteins by the diatom *Phaeodactylum tricornutum*. J Phycol 52:463–474

Callow JA, Callow ME (2011) Trends in the development of environmentally friendly fouling-resistant marine coatings. Nat Commun 2:244

Chen L, Weng D, Du C, Wang J, Cao S (2019) Contribution of frustules and mucilage trails to the mobility of diatom *Navicula* sp. Sci Rep 9:7342

Chiovitti A, Bacic A, Burke J, Wetherbee R (2003) Heterogeneous xylose-rich glycans are associated with extracellular glycoproteins from the biofouling diatom *Craspedostauros australis* (Bacillariophyceae). Eur J Phycol 38:351–360

Chiovitti A, Molino P, Crawford SA, Teng RW, Spurck T, Wetherbee R (2004) The glucans extracted with warm water from diatoms are mainly derived from intracellular chrysolaminaran and not extracellular polysaccharides. Eur J Phycol 39:117–128

Chiovitti A, Dugdale TM, Wetherbee R (2006) Diatom adhesives: molecular and mechanical properties. In: Smith AM, Callow J (eds) Biological adhesives. Springer, Berlin, pp 79–103

Chiovitti A, Heraud P, Dugdale TM, Hodson OM, Curtain RCA, Dagastine RR, Wood BR, Wetherbee R (2008) Divalent cations stabilize the aggregation of sulfated glycoproteins in the adhesive nanofibers of the biofouling diatom *Toxarium undulatum*. Soft Matter 4:811–820

Cohn SA (2001) Photo-stimulated effects on diatom motility. In: Häder DP, Lebert ML (eds) Comprehensive series in photosciences, vol 1. Elsevier, Amsterdam, pp 375–401

Cohn SA, Disparti NC (1992) Analysis of environmental-influences on diatom cell motility. Mol Biol Cell 3:A361–A361

Cohn SA, Disparti NC (1994) Environmental-factors influencing diatom cell motility. J Phycol 30: 818–828

Cohn SA, Weitzell RE (1996) Ecological considerations of diatom cell motility. I. Characterization of motility and adhesion in four diatom species. *J Phycol* 32:928–939

Cohn SA, Dunbar SA, Skoczylas C, Mucha JA (1997) Comparative analysis of diatom motility: phototactic behavior and sensitivity to ultraviolet radiation. Mol Biol Cell 8:2246

Cohn SA, Spurck TP, Pickett-Heaps JD (1999) High energy irradiation at the leading tip of moving diatoms causes rapid change of cell direction. Diatom Res 14:193–206

Cohn SA, Farrell J, Munro J, Rauschenberg C, Schulze J (2000) The effect of light and temperature on diatom aggregation and adhesion. *Mol Biol Cell* 11:381a

Cohn SA, Farrell JF, Munro JD, Ragland RL, Weitzell RE, Wibisono BL (2003) The effect of temperature and mixed species composition on diatom motility and adhesion. Diatom Res 18: 225–243

Cohn SA, Bahena M, Davis JT, Ragland RL, Rauschenberg CD, Smith BJ (2004) Characterisation of the diatom photophobic response to high irradiance. Diatom Res 19:167–179

Cohn SA, Halpin D, Hawley N, Ismail A, Kaplan Z, Kordes T, Kuhn J, Macke W, Marhaver K, Ness B, Olszewski S, Pike A, Rice E, Sbarboro J, Wolske A, Zapata Y (2015) Comparative analysis of light-stimulated motility responses in three diatom species. Diatom Res 30(3): 213–225

Cohn SA, Dunbar S, Ragland R, Schulze J, Suchar A, Weiss J, Wolske A (2016) Analysis of light quality and assemblage composition on diatom motility and accumulation rate. Diatom Res 31: 173–184

Consalvey M, Paterson DM, Underwood GJC (2004) The ups and downs of life in a benthic biofilm: Migration of benthic diatoms. Diatom Res 19:181–202

Cooksey B, Cooksey KE (1980) Calcium is necessary for motility in the diatom *Amphora coffeaeformis*. Plant Physiol 65:129–131

Cooksey B, Cooksey KE (1988) Chemical signal-response in diatoms of the genus Amphora. J Cell Sci 91:523–529

Crawford SA, Higgins MJ, Mulvaney P, Wetherbee R (2001) Nanostructure of the diatom frustule as revealed by atomic force and scanning electron microscopy. J Phycol 37:543–554

Croft MT, Lawrence AD, Raux-Deery E, Warren MJ, Smith AG (2005) Algae acquire vitamin B12 through a symbiotic relationship with bacteria. Nature 438:90–93

Daglio Y, Maidana NI, Matulewicz MC, Rodríguez MC (2016) Changes in motility and induction of enzymatic activity by nitrogen and phosphate deficiency in benthic *Halamphora luciae* (Bacillariophyceae) from Argentina. Phycologia 55:493–505

Daniel GF, Chamberlain AHL, Jones EBG (1980) Ultrastructural observations on the marine fouling Diatom *Amphora*. Helg Meeres 34:123–149

Daniel GF, Chamberlain AHL, Jones EBG (1987) Cytochemical and electron microscopical observations on the adhesive materials of marine fouling diatoms. Br Phycol J 22:101–118

de Brouwer JFC, Stal LJ (2001) Short-term dynamics in microphytobenthos distribution and associated extracellular carbohydrates in surface sediments of an intertidal mudflat. Mar Ecol Prog Ser 218:33–44

de Brouwer JFC, Stal LJ (2002) Daily fluctuations of exopolymers in cultures of the benthic diatoms *Cylindrotheca closterium* and *Nitzschia* sp (Bacillariophyceae). J Phycol 38:464–472

de Brouwer JFC, Wolfstein K, Ruddy GK, Jones TER, Stal LJ (2005) Biogenic stabilization of intertidal sediments: the importance of extracellular polymeric substances produced by benthic diatoms. Microb Ecol 49:501–512

Doiron K, Linossier I, Fay F, Yong J, Abd Wahid E, Hadjiev D, Bourgougnon N (2012) Dynamic approaches of mixed species biofilm formation using modern technologies. Mar Environ Res 78:40–47

Drum RW (1969) Light and electron microscope observations on the tube-dwelling diatom *Amphipleura rutilans* (trentepohl) Cleve. J Phycol L5:21–26

Drum RW, Hopkins JT (1966) Diatom locomotion - an explanation. Protoplasma 62:1–33

Du GY, Li WT, Li H, Chung IK (2012) Migratory responses of benthic diatoms to light and temperature monitored by chlorophyll fluorescence. J Plant Biol 55:159–164

Dugdale TM, Dagastine R, Chiovitti A, Mulvaney P, Wetherbee R (2005a) Single adhesive nanofibers from a live diatom have the signature fingerprint of modular proteins. Biophys J 89:4252–4260

Dugdale TM, Dagastine R, Chiovitti A, Wetherbee R (2005b) Utilizing the atomic force microscope to discern the structure and nano-mechanical properties of diatom adhesives. Phycologia 44:29

Dugdale TM, Dagastine R, Chiovitti A, Wetherbee R (2006a) Diatom adhesive mucilage contains distinct supramolecular assemblies of a single modular protein. Biophys J 90:2987–2993

Dugdale TM, Willis A, Wetherbee R (2006b) Adhesive modular proteins occur in the extracellular mucilage of the motile, pennate diatom *Phaeodactylum tricornutum*. Biophys J 90:58–60

Edgar LA (1979) Diatom locomotion: computer assisted analysis of cine film. Br Phycol J 14:83–101

Edgar LA (1982) Diatom Locomotion - a consideration of movement in a highly viscous situation. Br Phycol J 17:243–251

Edgar LA (1983) Mucilage secretions of moving diatoms. Protoplasma 118:44–48

Edgar LA, Pickett-Heaps JD (1982) Ultrastructural localization of polysaccharides in the motile diatom *Navicula cuspidata*. Protoplasma 113:10–22

Edgar LA, Pickett-Heaps JD (1983) The mechanism of diatom locomotion. I. An ultrastructural-study of the motility apparatus. *Proc R Soc B-Biological Sci* 218:331–343

Edgar LA, Pickett-Heaps J (1984) Diatom locomotion. In: Round FE, Chapman DJ (eds) Progress in phycological research. Biopress Ltd, Bristol, pp 47–88

Edgar LA, Zavortink M (1983) The mechanism of diatom locomotion. II. Identification of actin. *Proc R Soc B-Biological Sci* 218:345–348

Ezequiel J, Laviale M, Frankenbach S, Cartaxana P, Serôdio J (2015) Photoacclimation state determines the photobehaviour of motile microalgae: the case of a benthic diatom. J Exp Mar Biol Ecol 468:11–20

Figueroa FA, Abdala-Díaz A, Hernández V, Pedreros P, Aranda M, Cabrera-Pardo JR, Pérez C, Becerra J, Urrutia R (2020) Invasive diatom *Didymosphenia geminata* as a source of polysaccharides with antioxidant and immunomodulatory effects on macrophage cell lines. J Appl Phycol 32:93–102

Frankenbach S, Pais C, Martinez M, Laviale M, Ezequiel J, Serôdio J (2014) Evidence for gravitactic behaviour in benthic diatoms. Eur J Phycol 49:429–435

Gebeshuber IC, Kindt JH, Thompson JB, DelAmo Y, Stachelberger H, Brzezinski M, Stucky GD, Morse DE, Hansma PK (2000) Adhesives made by benthic diatoms studied by in vivo atomic force microscopy. *Biophys J* 78:10a

Gebeshuber IC, Thompson JB, Del Amo Y, Stachelberger H, Kindt JH (2002) In vivo nanoscale atomic force. Microscopy investigation of diatom adhesion properties. Mater Sci Technol 18: 763–766

Gebeshuber IC, Kindt JH, Thompson JB, Del Amo Y, Stachelberger H, Brzezinski M, Stucky GD, Morse DE, Hansma PK (2003) Atomic force microscopy study of living diatoms in ambient conditions. J Microsc 212:292–299

Gillard J, Frenkel J, Devos V, Sabbe K, Paul C, Rempt M, Inzé D, Pohnert G, Vuylsteke M, Vyverman W (2013) Metabolomics enables the structure elucidation of a diatom sex pheromone. Angew Chemie - Int Ed 52:854–857

Gordon R (1987) A retaliatory role for algal projectiles, with implications for the mechanochemistry of diatom gliding motility. J Theor Biol 126:419–436

Gordon R, Drum RW (1970) A capillarity mechanism for diatom gliding locomotion. Proc Natl Acad Sci U S A 67:338–344

Gretz M (2008) The stalks of didymo. In: Bothwell ML, Spaulding SA (eds) Proceedings of the 2007 International Workshop on *Didymosphenia geminata*. Canadian Technical Report on Fisheries and Aquatic Sciences 2795, p 21

Gupta S, Agrawal SC (2007) Survival and motility of diatoms *Navicula grimmei* and *Nitzschia palea* affected by some physical and chemical factors. Folia Microbiol (Praha) 52:127–134

Handel A (2017) Cell biology by the numbers. By Ron Milo and Rob Phillips. Garland Science (Taylor & Francis Group), New York

Harper MA (1967) Locomotion of diatoms and clumping of blue-green algae. Ph.D. Thesis, University of Bristol

Harper MA, Harper JF (1967) Measurements of diatom adhesion and their relationship with movement. Br Phycol Bull 3:195–207

Heintzelman MB, Enriquez ME (2010) Myosin diversity in the diatom *Phaeodactylum tricornutum*. Cytoskeleton 67:142–151

Helliwell KE, Chrachri A, Koester JA, Wharam S, Verret F, Taylor AR, Wheeler GL, Brownlee C (2019) Alternative mechanisms for fast Na +/Ca^{2+} signaling in eukaryotes via a novel class of single-domain voltage-gated channels. Curr Biol 29:319–321

Herm-Götz A, Weiss S, Stratmann R, Fujita-Becker S, Ruff C, Meyhöfer E, Soldati T, Manstein DJ, Geeves MA, Soldati D (2002) *Toxoplasma gondii* myosin A and its light chain: a fast, single-headed, plus-end-directed motor. EMBO J 21:2149–2158

Higashi-Fujime S, Ishikawa R, Iwasawa H, Kagami O, Kurimoto E, Kohama K, Hozumi T (1995) The fastest-actin-based motor protein from the green algae, Chara, and its distinct mode of interaction with actin. FEBS Lett 375:151–154

Higgins MJ, Crawford SA, Mulvaney P, Wetherbee R (2000) The topography of soft, adhesive diatom "trails" as observed by atomic force microscopy. Biofouling 16:133–139

Higgins MJ, Molino P, Mulvaney P, Wetherbee R (2003a) The structure and nanomechanical properties of the adhesive mucilage that mediates diatom-substratum adhesion and motility. J Phycol 39:1181–1193

Higgins MJ, Sader JE, Mulvaney P, Wetherbee R (2003b) Probing the surface of living diatoms with atomic force microscopy: the nanostructure and nanomechanical properties of the mucilage layer. J Phycol 39:722–734

Hoagland KD, Rosowski JR, Gretz MR, Roemer SC (1993) Diatom extracellular polymeric substances - function, fine-structure, chemistry, and physiology. J Phycol 29:537–566

Hodson OM, Monty JP, Molino PJ, Wetherbee R (2012) Novel whole cell adhesion assays of three isolates of the fouling diatom *Amphora coffeaeformis* reveal diverse responses to surfaces of different wettability. Biofouling 28:381–393

Holland R, Dugdale TM, Wetherbee R, Brennan AB, Finlay JA, Callow JA, Callow ME (2004) Adhesion and motility of fouling diatoms on a silicone elastomer. Biofouling 20:323–329

Hopkins JT (1963) A study of the diatoms of the Ouse Estuary, Sussex I The movement of the mud-flat diatoms in response to some chemical and physical changes. *J Mar Biol Assoc UK* 43: 653–663

Houpt PM (1994) Marine tube-dwelling diatoms and their occurrence in the Netherlands. Nether J Aqu Ecol 28:77–84

Idei M, Sato S, Tamotsu N, Mann DG (2018) Valve morphogenesis in *Diploneis smithii* (Bacillariophyta). J Phycol 54:171–186
Klapper F, Audoor S, Vyverman W, Pohnert G (2021) Pheromone mediated sexual reproduction of pennate diatom *Cylindrotheca closterium*. J Chem Ecol
Koedooder C, Stock W, Willems A, Mangelinckx S, De Troch M, Vyverman W, Sabbe K (2019) Diatom-bacteria interactions modulate the composition and productivity of benthic diatom biofilms. Front Microbiol 10:1255
Kooistra WHCF, De Stefano M, Mann DG, Salma N, Medlin LK (2003) Phylogenetic position of *Toxarium*, a pennate-like lineage within centric diatoms (Bacillariophyceae). J Phycologia 39: 185–197
Kriwy P, Uthicke S (2011) Microbial diversity in marine biofilms along a water quality gradient on the Great Barrier Reef. Syst Appl Microbiol 34:116–126
Lachnit M, Buhmann MT, Klemm J, Kröger N, Poulsen N (2019) Identification of proteins in the adhesive trails of the diatom *Amphora coffeaeformis*. Philos Trans R Soc B Biol Sci 374: 20190196
Larson C, Passy SI (2005) Spectral fingerprinting of algal communities: a novel approach to biofilm analysis and biomonitoring. J Phycol 41:439–446
Lauterborn R (1896) Untersuchungen über bau, kernteilung und bewegung der diatomeen, 165 p. Engelmann, Leipzig
Lawrence JR, Swerhone GDW, Leppard GG, Araki T, Zhang X, West MM, Hitchcock AP (2003) Scanning transmission X-ray, laser scanning, and transmission electron microscopy mapping of the exopolymeric matrix of microbial biofilms. Appl Environ Microbiol 69:5543–5554
Le Norcy T, Faÿ F, Obando CZ, Hellio C, Réhel K, Linossier I (2019) A new method for evaluation of antifouling activity of molecules against microalgal biofilms using confocal laser scanning microscopy-microfluidic flow-cells. Int Biodeterior Biodegrad 139:54–61
Lewin RA (1958) The mucilage tubes of *Amphipleura rutilans*. Limnol Oceanogr 3:111–113
Lind JL, Heimann K, Miller EA, Van Vliet C, Hoogenraad NJ, Wetherbee R (1997) Substratum adhesion and gliding in a diatom are mediated by extracellular proteoglycans. Planta 203:213–221
Mann DG (1985) In vivo observations of plastid and cell division in raphid diatoms and their relevance to diatom systematics. Ann Bot 55:95–108
Mann DG (1989) The diatom genus Sellaphora: Separation from Navicula. Br Phycol J 24:1–20
Massé G, Poulin M, Belt ST, Robert JM, Barreau A, Rincé Y, Rowland SJ (2001) A simple method for SEM examination of sectioned diatom frustules. J Microsc 204:87–92
McConville MJ, Wetherbee R, Bacic A (1999) Subcellular location and composition of the wall and secreted extracellular sulphated polysaccharides/proteoglycans of the diatom *Stauroneis amphioxys* Gregory. Protoplasma 206:188–200
McLachlan DH, Brownlee C, Taylor AR, Geider RJ, Underwood GJC (2009) Light-induced motile responses of the estuarine benthic diatoms *Navicula perminuta* and *Cylindrotheca closterium* (Bacillariophyceae). J Phycol 45:592–599
McLachlan DH, Underwood GJC, Taylor AR, Brownlee C (2012) Calcium release from intracellular stores is necessary for the photophobic response in the benthic diatom *Navicula perminuta* (Bacillariophyceae). J Phycol 48:675–681
Mock T, Otillar R, Strauss J et al (2017) Evolutionary genomics of the cold-adapted diatom *Fragilariopsis cylindrus*. Nature 541:536–540
Molino PJ, Wetherbee R (2008) The biology of biofouling diatoms and their role in the development of microbial slimes. Biofouling 24:365–379
Molino PJ, Hodson OM, Quinn JF, Wetherbee R (2006) Utilizing QCM-D to characterize the adhesive mucilage secreted by two marine diatom species in-situ and in real-time. Biomacromolecules 7:3276–3282
Moss JA, Nocker A, Lepo JE, Snyder RA (2006) Stability and change in estuarine biofilm bacterial community diversity. Appl Environ Microbiol 72:5679–5688
Müller O (1893) Die Ortsbewegung der Bacillariaceen betreffend I. Ber Dtsch Bot Ges 11:571–576

Neu T, Kuhlicke U (2017) Fluorescence lectin bar-coding of glycoconjugates in the extracellular matrix of biofilm and bioaggregate forming microorganisms. Microorganisms 5:5
Nultsch W (1971) Phototactic and photokinetic action spectra of the diatom *Nitzschia communis*. Photochem Photobiol 14:705–712
Nultsch W, Häder DP (1988) Photomovement in motile microorganisms—II. Photochem Photobiol 47:837–869
Osuna-Cruz CM, Bilcke G, Vancaester E et al (2020) The *Seminavis robusta* genome provides insights into the evolutionary adaptations of benthic diatoms. Nat Commun 11:3320
Paterson DM (1986) The migratory behaviour of diatom assemblages in a laboratory tidal scanning electron microscopy micro-ecosystem examined by low temperature. Diatom Res 1:227–239
Paul C, Pohnert G (2011) Interactions of the algicidal bacterium *Kordia algicida* with diatoms: Regulated protease excretion for specific algal lysis. PLoS One 6:e21032
Perkins RG, Lavaud J, Serôdio J, Mouget JL, Cartaxana P, Rosa P, Rosa P, Barille L, Brotas V, Jesus BM (2010) Vertical cell movement is a primary response of intertidal benthic biofilms to increasing light dose. Mar Ecol Prog Ser 416:93–103
Pickett-Heaps J, Hill DRA, Blaze KL (1991) Active gliding motility in an araphid marine diatom, *Ardissonea* (Formerly Synedra) *crystallina*. J Phycol 27:718–725
Pierobon P, Achouri S, Courty S, Dunn AR, Spudich JA, Dahan M, Cappello G (2009) Velocity, processivity, and individual steps of single myosin V molecules in live cells. Biophys J 96: 4268–4275
Poulsen NC, Spector I, Spurck TP, Schultz TF, Wetherbee R (1999) Diatom gliding is the result of an actin-myosin motility system. Cell Motil Cytoskeleton 44:23–33
Poulsen N, Kröger N, Harrington MJ, Brunner E, Paasch S, Buhmann MT (2014) Isolation and biochemical characterization of underwater adhesives from diatoms. Biofouling 30:513–523
Prins A, Deleris P, Hubas C, Jesus B (2020) Effect of light intensity and light quality on diatom behavioral and physiological photoprotection. Front Mar Sci 7:203
Rastogi K, Puliyakodan MS, Pandey V, Nath S, Elangovan R (2016) Maximum limit to the number of myosin II motors participating in processive sliding of actin. Sci Rep 6:32043
Rogers JD, Perreault NN, Niederberger TD, Lichten C, Whyte LG, Nadeau JL (2010) A life detection problem in a High Arctic microbial community. Planet Space Sci 58:623–630
Sato S, Medlin LK (2006) Motility of non-raphid diatoms. Diatom Res 21:473–477
Sauer J, Wenderoth K, Maier UG, Rhiel E (2002) Effects of salinity, light and time on the vertical migration of diatom assemblages. Diatom Res 17:189–203
Scardino AJ, Harvey E, De Nys R (2006) Testing attachment point theory: diatom attachment on microtextured polyimide biomimics. Biofouling 22:55–60
Schultz MP, Bendick JA, Holm ER, Hertel WM (2011) Economic impact of biofouling on a naval surface ship. Biofouling 27:87–98
Serôdio J, Vieira S, Cruz S (2008) Photosynthetic activity, photoprotection and photoinhibition in intertidal microphytobenthos as studied in situ using variable chlorophyll fluorescence. Cont Shelf Res 28:1363–1375
Smith DJ, Underwood GJC (1998) Exopolymer production by intertidal epipelic diatoms. Limnol Oceanogr 43:1578–1591
Spaulding SA, Elwell L (2007) Increase in nuisance blooms and geographic expansion of the freshwater diatom Didym*osphenia geminata*. In: U.S. Geological Survey Open-File Report 2007–1425, 38 p
Staats N, De Winder B, Stal LJ, Mur LR (1999) Isolation and characterization of extracellular polysaccharides from the epipelic diatoms *Cylindrotheca closterium* and *Navicula salinarum*. Eur J Phycol 34:161–169
Staats N, Stal LJ, de Winder B, Mur LR (2000a) Oxygenic photosynthesis as driving process in exopolysaccharide production of benthic diatoms. Mar Ecol Ser 193:261–269
Staats N, Stal LJ, Mur LR (2000b) Exopolysaccharide production by the epipelic diatom *Cylindrotheca closterium*: effects of nutrient conditions. J Exp Mar Bio Ecol 249:13–27

Stal LJ (2010) Microphytobenthos as a biogeomorphological force in intertidal sediment stabilization. Ecol Eng 36:236–245

Sweeney HL, Houdusse A (2010) Myosin VI rewrites the rules for myosin motors. Cell 141:573–582

Underwood GJC (2010) Exopolymers (extracellular polymeric substances) in diatom-dominated marine sediment biofilms. In: Seckbach J, Oren A (eds) Microbial Mats, *Cellular origin, life in extreme habitats and astrobiology*, vol 14. Springer, Dordrecht, pp 287–300

Underwood GJC, Boulcott M, Raines CA, Waldron K (2004) Environmental effects on exopolymer production by marine benthic diatoms: dynamics, changes in composition, and pathways of production. J Phycol 40:293–304

Underwood GJC, Perkins RG, Consalvey MC, Hanlon ARM, Oxborough K, Baker NR, Paterson DM (2005) Patterns in microphytobenthic primary productivity: species-specific variation in migratory rhythms and photosynthetic efficiency in mixed-species biofilms. Limnol Oceanog 50:755–767

Underwood GJC, Fietz S, Papadimitriou S, Thomas DN, Dieckmann GS (2010) Distribution and composition of dissolved extracellular polymeric substances (EPS) in Antarctic sea ice. Mar Ecol Prog Ser 404:1–19

Villacorte LO, Ekowati Y, Neu TR, Kleijn JM, Winters H, Amy G, Schippers JC, Kennedy MD (2015) Characterisation of algal organic matter produced by bloom-forming marine and freshwater algae. Water Res 73:216–230

Wang Y, Lu JJ, Mollet JC, Gretz MR, Hoagland KD (1997) Extracellular matrix assembly in diatoms (Bacillariophyceae) .2. 2,6-dichlorobenzonitrile inhibition of motility and stalk production in the marine diatom *Achnanthes longipes*. Plant Physiol 113:1071–1080

Wang Y, Chen Y, Lavin C, Gretz MR (2000) Extracellular matrix assembly in diatoms (Bacillariophyceae). IV Ultrastructure of Achnanthes longipes and Cymbella cistula as revealed by high-pressure freezing/freeze substituton and cryo-field emission scanning electron microscopy. *J Phycol* 36:367–378

Wang J, Cao S, Du C, Darong C (2013) Underwater locomotion strategy by a benthic pennate diatom *Navicula* sp. Protoplasma 250:1203–1212

Webster DR, Cooksey KE, Rubin RW (1985) An investigation of the involvement of cytoskeletal structures and secretion in gliding motility of the marine diatom, Amphora coffeaeformis. Cell Motil Cytoskeleton 5:103–122

Wetherbee R, Lind JL, Burke J, Quatrano RS (1998) The first kiss: establishment and control of initial adhesion by raphid diatoms. J Phycol 34:9–15

Whitton BA, Ellwood NTW, Kawecka B (2009) Biology of the freshwater diatom Didymosphenia: a review. Hydrobiologia 630:1–37

Wigglesworth-Cooksey B, Cooksey KE (2005) Use of fluorophore-conjugated lectins to study cell-cell interactions in model marine biofilms. Appl Environ Microbiol 71:428–435

Willis A, Chiovitti A, Dugdale TM, Wetherbee R (2013) Characterization of the extracellular matrix of *Phaeodactylum tricornutum* (Bacillariophyceae): structure, compostion and adhesive characteristics. J Phycol 49:937–949

Willis A, Eason-Hubbard M, Hodson O, Maheswari U, Bowler C, Wetherbee R (2014) Adhesion molecules from the diatom *Phaeodactylum tricornutum* (Bacillariophyceae): genomic identification by amino-acid profiling and in vivo analysis. J Phycol 50:837–849

Windler M, Leinweber K, Bartulos CR, Philipp B, Kroth PG (2015) Biofilm and capsule formation of the diatom *Achnanthidium minutissimum* are affected by a bacterium. J Phycol 51:343–355

Wustman BA, Gretz MR, Hoagland KD (1997) Extracellular matrix assembly in diatoms (Bacillariophyceae). 1. A model of adhesives based on chemical characterization and localization of polysaccharides from the marine diatom *Achnanthes longipes* and other diatoms. Plant Physiol 113:1059–1069

Wustman BA, Lind J, Wetherbee R, Gretz MR (1998) Extracellular matrix assembly in diatoms - (Bacillariophyceae) – III. Organization of fucoglucuronogalactans within the adhesive stalks of *Achnanthes longipes*. *Plant Physiol* 116:1431–1441